produces a decrease in the surface hydroxyl coverage of ~50-60%, whereas the 4-*tert*-butylpyridine exposure alone produces a decrease of ~15-20%. This suggests that, in fact, the MoO_2Cl_2 reacted with the surface hydroxyl groups to form the molybdenum oxide surface and desorb the hydroxyl protons as HCl. The 4-*tert*-butylpyridine then reacted with the oligomerized molybdenum oxide and desorbed the molybdenum oxide from the surface.

Nitrogen-containing bases (e.g., diethylenetriamine) are sufficiently strong to produce depolymerization of molybdenum oxide.[32] This suggests the reaction sequence

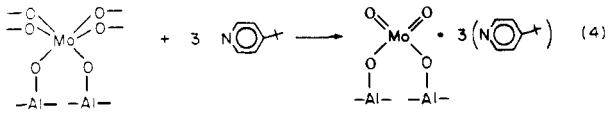

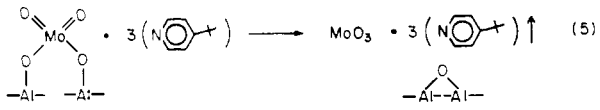

The ratio of three molecules of 4-*tert*-butylpyridine to one molecule of MoO_3 is hypothetical, but it is based on the observed octahedral coordination of MoO_3 with three basic sites for ligands. There is more than sufficient 4-*tert*-butylpyridine present in the system to satisfy the proposed stoichiometry.

The extremely strong reaction of the molybdenum oxide with Lewis bases suggests that further investigations with weaker bases or much lower exposures may produce data complementing the primarily Brønsted acid nature of adsorbates on hydroxylated aluminum oxide. In addition, molybdenum oxide is used widely as a catalyst for oxidation reactions either by itself or in the form of a mixed oxide.[21] The availability of relatively volatile (e.g., vapor pressure $>10^{-2}$ Torr) halogen or other salts of many metals suggests the possibility of generalizing this method of oxide generation to other metal systems and the formation of mixed metal oxide surfaces. Finally, the availability of dehydroxylated alumina surfaces provides the opportunity for comparison with the hydroxylated alumina surfaces used heretofore in tunneling spectroscopy.

V. Conclusions

The reaction of $MoOCl_4$ with the hydroxylated alumina surface produces a probable dimeric, oxygen-bridged surface species analogous to dimeric MoO_2Cl_2. This species is unstable with respect to desorption under vacuum. Heating the surface during exposure to $MoOCl_4$ produces a molybdenum oxide surface that is poorly suited to tunneling spectroscopy.

Reacting MoO_2Cl_2 with the hydroxylated alumina surface produces a series of molybdenum oxide surface species. The degree of oligomerization depends on the extent of heating. Surface species which have not been post-heated under vacuum give spectral evidence for adsorbed water and molybdenum hydroxide formation. Post-heating removes the chemisorbed water.

The molybdenum oxide surface displays little reactivity toward ethylene exposed at 100 °C. The molybdenum oxide surface causes decomposition of acetic acid adsorbed at 22 °C. The oxide reacts with 4-*tert*-butylpyridine, present in substantial excess, causing desorption of the molybdenum oxide, possibly as a volatile $MoO_3 \cdot 3$(pyridine) complex. The resulting surface is dehydroxylated aluminum oxide.

The use of volatile metal oxochlorides to form suitable metal oxide surfaces for study by tunneling spectroscopy has been established. Future work on molybdenum and other metal oxide surfaces formed by halide hydrolysis, as well as the availability of dehydroxylated alumina surfaces, has the potential to expand significantly the variety of surfaces capable of being studied by inelastic electron-tunneling spectroscopy.

Acknowledgment. This research was supported by the National Science Foundation under Grant No. DMR-8500789.

Rotational Spectra and Structures of the Small Clusters Ar_3-HF and Ar_3-DF

H. S. Gutowsky,* T. D. Klots, Carl Chuang, John D. Keen, C. A. Schmuttenmaer, and Tryggvi Emilsson

Contribution from the Noyes Chemical Laboratory, University of Illinois, Urbana, Illinois 61801. *Received February 13, 1987*

Abstract: Microwave rotational spectra have been observed for the two small clusters $^{40}Ar_3$-HF and $^{40}Ar_3$-DF, the first clusters to be so characterized. Their detection was made possible by sensitivity improvements to a Flygare spectrometer, which uses Fourier transform operation of a Fabry-Perot microwave cavity in conjunction with a pulsed supersonic nozzle to generate the clusters. The symmetric top transitions measured for $J = 1 \rightarrow 2$ to $J = 6 \rightarrow 7$ are fitted by rotational constants B_0, D_J, and D_{JK} of 1188.212 MHz, 6.85 kHz, and -5.76 kHz for Ar_3-HF and of 1180.379 MHz, 6.57 kHz, and -5.156 kHz for Ar_3-DF. The composition and C_{3v} symmetry of the clusters were established by the conditions of their formation, by the hyperfine structure of their transitions, by the absence of K states other than 0, ±3, and ±6, and by analysis of the values found for B_0. The H/DF lies along the threefold axis of the Ar_3 group, with the H/D end closest to Ar_3. Analysis of the moments of inertia and torsional amplitudes for the two isotopic species gives an approximate Ar_3 c.m. to HF c.m. distance of 2.735 Å and an estimate of 3.835 Å for the Ar-Ar distance. Tilt of the Ar_3 group is considered in the estimate. The Ar to HF c.m. and Ar-Ar distances in the clusters are comparable with those in the Ar_2 and Ar-HF dimers and Ar_2-HF trimer. The shape of the interaction potential between Ar_3 and the H/DF is discussed.

During the past 15 years pure rotational spectra have been studied for the ground vibrational state of a considerable number and variety of dimers formed by hydrogen bonding or van der Waals forces.[1] The more strongly hydrogen-bonded species have been investigated by Stark-modulation microwave spectroscopy of cooled gas mixtures at equilibrium.[1] Two experimental approaches have been employed for the more weakly bonded species, both previously limited to the study of dimers[2]—the molecular beam electric resonance method of the Klemperer group,[3] and

(1) Legon, A. C.; Millen, D. J. *Chem. Rev.* **1986**, *86*, 635.

(2) See, for example, Leopold, K. R. (Ph.D. Thesis, Harvard University, 1983), who describes an inconclusive search for Ar_2-OCS.

(3) Bowen, K. H., Jr. Ph.D. Thesis, Harvard University, 1977. Dyke, T. R.; Tomasevich, G. R.; Klemperer, W. *J. Chem. Phys.* **1972**, *57*, 2277.

0002-7863/87/1509-5633$01.50/0

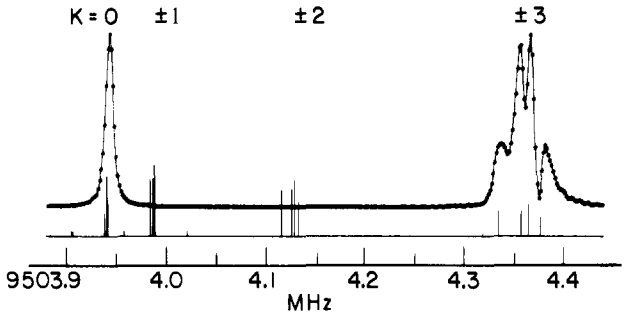

Figure 1. Centrifugal distortion and hyperfine structure of the $J = 3 \rightarrow 4$ rotational transition of Ar_3–HF. The observed spectrum (top) is a composite of two overlapping parts. The $K = 0$ portion was obtained in 3.8 min by averaging 1818 FIDs digitized at 300 ns for 512 points, giving a resolution of 1.628 kHz/point. The $K = \pm 3$ portion is the average of 1765 FIDs, obtained in 3.6 min. The Doppler doubling has been suppressed. The stick spectrum (bottom) was calculated with the rotational parameters given in Table IV.

the Flygare–Balle Fourier transform spectrometer with a pulsed nozzle.[4] Recently we extended the latter technique to the study of small clusters, in particular to the tetramers Ar_3–HF and –DF for which a preliminary account was published,[5] and to the T-shaped trimers Ar_2–H/DF[6] and Ar_2–$H^{35}Cl/^{37}Cl$ that have just been described more fully.[7]

Herein we present the details of our earlier work on the small clusters Ar_3–HF and –DF, in their ground vibrational state, and provide some additional results that support our initial characterization of these interesting new species. Our studies have shown them to be oblate symmetric tops with a threefold symmetry axis. They can perhaps best be described as an equilateral argon trimer with an HF lying along the principal axis, attracted symmetrically to all three argons. The HF is loosely bound and makes large amplitude (~40°) torsional oscillations about the c axis. The dimensions and internal dynamics of the tetramers are comparable with those found for the Ar_2–H/DF trimers[6] and Ar–H/DF dimers.[8,9]

Experimental Section

The rotational spectra were observed with the Flygare–Balle Mark II spectrometer.[10] In it a microwave pulse is applied to an evacuated Fabry–Perot cavity tuned to that frequency, synchronized with a pulsed jet of a gas mixture from a supersonic nozzle. The gas is cooled to ~5 K by the expansion which generates a variety of molecular complexes.[3] A molecular free induction decay (FID) appears in the cavity after the microwave pulse when the microwave frequency is with ~0.5 MHz of a rotational transition. The FID is detected, digitized and recorded, averaged for a number of microwave and gas pulses, and Fourier transformed to give the power spectrum an example of which is shown in Figure 1.

Observation of the Ar_3–H/DF clusters was accomplished by several improvements in the spectrometer which better utilize its potential sensitivity.[5,6] In most of the measurements argon was used as the carrier gas, with 0.5 to 1.0% of HF and/or DF added. The nozzle was 0.94 mm in diameter. The backing pressure of the gas mixture was ~1 atm, and it was at ambient temperature. The HF was supplied by Linde; the DF was synthesized locally by reduction of $KCuF_3$ with D_2, by thermal decomposition of KDF_2, and by reaction of D_2 with F_2.

Table I. Observed and Calculated Frequencies of the Rotational Line Centers for Ar_3–HF[a]

$J,K \rightarrow J',K'$	obsd. MHz	calcd, MHz	diff, kHz
1,0 → 2,0	4752.628	4752.630	−2
2,0 → 3,0	7128.533	7128.534	−1
3,0 → 4,0	9503.944	9503.946	−2
3,±3 → 4,±3	4.359	4.360	−1
4,0 → 5,0	11878.699	11878.700	−1
4,±3 → 5,±3	9.219	9.218	2
5,0 → 6,0	14252.636	14252.632	4
5,±3 → 6,±3	3.257	3.254	3
6,0 → 7,0	16625.579	16625.579	0
6,±3 → 7,±3	6.300	6.304	−4
6,±6 → 7,±6	8.479	8.479	0

[a] Transition frequencies for states with $K \neq 0$ are emphasized by omitting the first 3 or 4 digits, which are the same as for the transition just above.

Table II. Observed and Calculated Frequencies of the Rotational Line Centers for Ar_3–DF[a]

$J,K \rightarrow J',K'$	obsd, MHz	calcd, MHz	diff, kHz
1,0 → 2,0	4721.304	4721.304	0
3,0 → 4,0	9441.346	9441.347	−1
3,±3 → 4,±3	1.74[b]	1.718	
4,0 → 5,0	11800.502	11800.502	0
4,±3 → 5,±3	0.96[b]	0.965	
5,0 → 6,0	14158.872	14158.869	3
5,±3 → 6,±3	9.44[b]	9.425	
6,0 → 7,0	16516.288	16516.291	−3
6,±3 → 7,±3	6.941	6.939	2
6,±6 → 7,±6	8.882	8.883	−1

[a] Transition frequencies for states with $K \neq 0$ are emphasized by omitting the first 3 or 4 digits, which are the same as for the transition just above. [b] Approximate center of partially resolved hyperfine structure; not used in determination of rotational constants.

Recent experiments were designed to resolve the hyperfine structure (hfs) of the $K = \pm 3$, $J = 3 \rightarrow 4$ transition of Ar_3–HF (Figure 1) and to show directly that argon is a constituent of the complexes observed. We have achieved better resolution by suppressing the usual Doppler broadening and doubling of transitions observed with the spectrometer.[4] In the present case, this was done by using a Laval type nozzle with a skimmer.[11] The nozzle consists of a cone through a thin plate (2.5 mm thick) with an inlet diameter of 0.5 mm and an outlet to the cavity of 3.0 mm, the plate screwed to the face of the valve (General Valve Co.). Although the cone is not a true Laval nozzle it does reduce the Doppler doubling and provides narrower lines. Its performance was improved by use of a skimmer, each half of which was at an angle of 30° with respect to the axis of the gas jet. In Figure 1, the full width at half maximum amplitude of the $K = 0$ line is 9 kHz.

Assignment of the transitions to species containing argon was verified by experiments in which the carrier gas was changed from argon to first run neon (Airco).[11] The latter consists of 70% neon and 30% helium; it was used at a backing pressure of ~2 atm. With it we have found several-fold increases in signal strength for other complexes of current interest to our group, e.g., diborane–HCl, Ar_2–HCl, and Ar_3–HCl, though not for $(HCN)_3$ or trimers containing $(HCN)_2$. Addition of both HF and argon to the first run neon was necessary to observe the $J = 4 \rightarrow 5$ transitions at 11879 MHz attributed to Ar_3–HF. Furthermore the signal strengths for the symmetric top transitions were approximately a quarter of those for Ar_2–HF,[6] in rough agreement with the ratio of Ar_3 to Ar_2 formation in the nozzle expansion.[3]

In the measurements, several Fourier transforms were recorded at different excitation frequencies for each transition, $J,K \rightarrow J+1,K$. Its frequency or those of any well-resolved hfs were measured and averaged. The standard deviation of the average reported for a well-resolved component is typically 1 kHz, including the calibration uncertainty.

Results and Analysis

Line Centers. The results of our measurements are given in Tables I–III. They are very similar for the HF and DF species. There is a uniform difference of 0.66% in the frequencies of the line centers for the two species. Also, where hyperfine structure (hfs) is found, that for DF extends over nearly twice the range

(4) Balle, T. J.; Flygare, W. H. *Rev. Sci. Instrum.* **1981**, *52*, 33. Campbell, E. J.; Buxton, L. W.; Balle, T. J.; Keenan, M. R.; Flygare, W. H. *J. Chem. Phys.* **1981**, *74*, 829.

(5) Gutowsky, H. S.; Klots, T. D.; Chuang, C.; Keen, J. D.; Schmuttenmaer, C. A.; Emilsson, T. I. *J. Am. Chem. Soc.* **1985**, *107*, 7174.

(6) Gutowsky, H. S.; Klots, T. D.; Chuang, C.; Schmuttenmaer, C. A.; Emilsson, T. *J. Chem. Phys.* **1985**, *83*, 4817; **1987**, *86*, 569.

(7) Klots, T. D.; Chuang, C.; Ruoff, R. S.; Emilsson, T.; Gutowsky, H. S. *J. Chem. Phys.* **1987**, *86*, 5315.

(8) Dixon, T. A.; Joyner, C. H.; Baiocchi, F. A.; Klemperer, W. J. *Chem. Phys.* **1981**, *74*, 6539.

(9) Keenan, M. R.; Buxton, L. W.; Campbell, E. J.; Legon, A. C.; Flygare, W. H. *J. Chem. Phys.* **1981**, *74*, 2133. For the value of D_0(HF) see also: Shea, J. A.; Flygare, W. H. *J. Chem. Phys.* **1982**, *76*, 4857.

(10) Campbell, E. J.; Read, W. G.; Shea, J. A. *Chem. Phys. Lett.* **1983**, *94*, 69.

(11) Ruoff, R. S.; Emilsson, T.; Klots, T. D.; Chuang, C.; Gutowsky, H. S. *J. Chem. Phys.*, in press.

Table III. Observed and Calculated Frequencies of the Hyperfine Components in the $K = 0$, $J = 1 \rightarrow 2$ Transitions of Ar_3-HF and Ar_3-DF and in the $K = \pm 3$, $J = 3 \rightarrow 4$ Transition of Ar_3-HF

components		obsd,[a]	calcd,[a]	diff,
$J,F_1,F \rightarrow$	J',F_1',F'	MHz	MHz	kHz
$J = 1 \rightarrow 2$ Transition at 4752.628 MHz for HF Species				
$1,^3/_2,2$	$2,^3/_2,2$	2.597	2.597	0
$1,^1/_2,0$	$2,^3/_2,1$	2.603	2.602	1
$1,^1/_2,1$	$2,^3/_2,2$	2.628	2.628	0
$1,^3/_2,1$	$2,^5/_2,2$		2.628	0
$1,^3/_2,2$	$2,^5/_2,3$		2.630	-2
$1,^1/_2,1$	$2,^3/_2,1$	2.679	2.678	1
$J = 1 \rightarrow 2$ Transition at 4721.304 MHz for DF Species				
$1,1,^3/_2$	$2,1,^3/_2$	1.215	1.216	-1
$1,1,^1/_2$	$2,2,^3/_2$	1.300	1.298	2
$1,2,^3/_2$	$2,3,^5/_2$		1.299	1
$1,2,^5/_2$	$2,3,^7/_2$		1.301	-1
$1,1,^3/_2$	$2,2,^5/_2$	1.307	1.306	1
$1,0,^1/_2$	$2,1,^3/_2$	1.341	1.343	-2
$J = 3 \rightarrow 4$, $K = \pm 3$ Transition at 9504.359 MHz for HF Species				
3,1,3[b]	4,1,4[b]	4.335	4.334	1
3,0,3	4,0,4	4.354	4.357	-3
3,1,4	4,1,5	4.365	4.365	0
3,1,2	4,1,3	4.380	4.376	4

[a] The first 3 digits of the frequencies are omitted. [b] Here the middle digit is $I = I_H + I_F$.

for HF (Table III). For each species there is a series of nearly equally spaced (~2370 MHz) transitions; those at higher J (3 to 7) are split into two or three different components by the K-dependent centrifugal distortion. In most cases the line center is simply the frequency of maximum intenstiy, i.e., the average of a Doppler doublet. The transitions for $K = 0$ are narrow, strong lines except for $J = 1 \rightarrow 2$, which exhibits weak satellites from the H/DF hyperfine interactions. These were fitted to obtain the line center, as given in Table III. The $J = 0 \rightarrow 1$ transitions (~2370 MHz) are below the present operating range of the spectrometer. For Ar_3-HF, the $K = \pm 3$ transitions for $J = 3 \rightarrow 4$ and $4 \rightarrow 5$ have appreciable hfs; that for $J = 3 \rightarrow 4$ was resolved and fitted as described in the next section. For Ar_3-DF the hfs of the $K = \pm 3$ transitions is more extensive and only approximate line centers are given for $J = 3 \rightarrow 4$, $4 \rightarrow 5$, and $5 \rightarrow 6$.

The other line centers are fitted quite accurately by the usual expression for the frequency of the $J \rightarrow J + 1$, $\Delta K = 0$ transitions in a symmetric top:[12]

$$\nu = 2B_0(J + 1) - 4D_J(J + 1)^3 - 2D_{JK}(J + 1)K^2 \quad (1)$$

The first two terms describe the $K = 0$ transitions and the last term the $|K| > 0$. The components associated with the K-dependent centrifugal distortion D_{JK} have a characteristic pattern indicating that only K states which are integral multiples of three occur for both the HF and DF species. As shown in Tables I and II, we found only the $K = 0$ transitions for $J = 1 \rightarrow 2$ and $2 \rightarrow 3$. Then, for the $J = 3 \rightarrow 4$, $4 \rightarrow 5$, and $5 \rightarrow 6$ transitions, there is only one D_{JK}-dependent component. Finally, for $J = 6 \rightarrow 7$, there are two such components. This behavior is predicted[12] for symmetric tops with a threefold symmetry axis which interchanges identical $I = 0$ nuclei. The most abundant species in the system by far is ^{40}Ar, with spin zero and 99.6% abundance, so we have assigned the D_{JK}-dependent components as $K = \pm 3$ and ± 6.[13] An alternate assignment is as $K = \pm 1$ and ± 2, with the higher K states too weak for detection. However, this would raise the question of why the $K = \pm 1$ state was observed for $J \geq 3$ but not below and the $K = \pm 2$ state for $J \geq 6$ but not below. The results of fitting eq 1 to the line centers with a nonlinear least-squares program are listed in Table IV for the preferred assignment. The alternate assignment gives the same fit except that D_{JK} is ninefold (3^2) larger.

(12) Townes, C. H.; Schawlow, A. L. *Microwave Spectroscopy*; McGraw-Hill; New York, 1955; pp 48-82 and 149-173.

(13) We thank W. Klemperer for helping us mind our J's and K's.

Hyperfine Structure. Most of the intensity for the $J = 1 \rightarrow 2$ transitions of the symmetric tops is in a central set of unresolved components; however, we were able to measure several weak outer satellites (Table III). The observed patterns resemble closely the H/DF hyperfine structure reported previously by Keenan et al.[9] for the $J = 1 \rightarrow 2$ transitions of Ar-H/DF. The hyperfine interactions for the $K = 0$, $J \rightarrow J + 1$ transitions of a symmetric top with an H/DF along its figure axis are the same as for the linear Ar-H/DF dimers, so we[12] fitted the hfs in the same manner. Spin-rotation was neglected and the Hamiltonian included only the rotational (H_R) and dipole-dipole interaction (H_D) terms for Ar_3-HF with addition of the deuterium quadrupole term (H_Q) for Ar_3-DF. The matrix elements were calculated for Ar_3-HF with the basis set

$$J + I_F = F_1,\ F_1 + I_H = F \quad (2)$$

and for Ar_3-DF with

$$J + I_D = F_1,\ F_1 + I_F = F \quad (3)$$

The hfs observed for the $J = 1 \rightarrow 2$ transitions was fitted with a nonlinear least-squares procedure. The adjustable parameters are the line center and the projections D_c and χ_c along the c inertial axis of the dipole-dipole and deuterium nuclear quadrupole interactions, respectively.[9] With the usual approximation that the structure of free H/DF is preserved in the complex, D_c is given by

$$D_c = (D_0/2)\langle 3\cos^2\theta - 1\rangle \quad (4)$$

with a similar equation for χ_c. D_0 and χ_0 are the interaction constants in free H/DF and θ is the angle between the H/DF and the c axis. The fit obtained in this manner is given in Table III; it is comparable with that for the $J = 0 \rightarrow 1$ transitions of Ar-H/DF.[9] The values found for D_c and χ_c are included in Table IV; they were used to solve eq 4 for the "average" torsional angle θ, also given there. Angles of 41.0 and 35.6° are obtained in this manner for Ar_3-H/DF while those reported for a similar analysis of Ar-H/DF are 41.6 and 33.5°.[9] If the difference in torsional angles for HF and DF is only a mass effect, their ratio should be $(\mu_{DF}/\mu_{HF})^{1/4} = 1.175$ in the harmonic oscillator approximation, where μ is the reduced mass. The ratio observed for Ar_3-H/DF is 1.152 and that for Ar-H/DF is 1.242. There is no evidence of perturbations from other $I \neq 0$ nuclei, and the hfs establishes the presence of an H/DF molecule at the figure axis of the symmetric top.

As a check on our assignment of the K states, we resolved and fitted the hf and centrifugal distortion structure in the $J = 3 \rightarrow 4$ transitions of Ar_3-HF, the lowest J for which we have found more than the $K = 0$ transition. The observed spectrum is reproduced at the top of Figure 1, which is a composite of the $K = 0$ singlet at 9503.944 MHz and a quartet centered at the higher frequency, 9504.359 MHz. The full set of possible transitions and hfs for $J = 3 \rightarrow 4$ was calculated with the same, general 2-spin program we used for Ar_2-H/DF.[6,14] Spin-rotation was neglected and matrix elements of the Hamiltonian, $H = H_R + H_D$, were determined by applying tensor methods to the basis set

$$I_H + I_F = I,\ I + J = F \quad (5)$$

The stick spectrum at the bottom of Figure 1 was calculated in this manner with the parameters given for Ar_3-HF in Table IV.

The calculated spectrum consists of four sets of hfs, for $K = 0, \pm 1, \pm 2$, and ± 3. Each set has four main components, the spread of which increases monotonically from ~4 kHz for $K = 0$ to 42 kHz for $K = \pm 3$. The observed spectrum is in excellent agreement with the predictions for $K = 0$ and ± 3. The numerical results for $K = \pm 3$ are compared in Table III. The frequencies predicted for rotational states with $|K| > 0$ depend of course upon the assignment of the observed states, so the agreement in "observed" and calculated line centers for $K = \pm 3$ does not in itself confirm the assignment. However, the spread of the hfs, while depending on both J and K, is not affected by D_{JK} or D_J but is determined

(14) Read, W. G.; Flygare, W. H. *J. Chem. Phys.* **1982**, *76*, 2238.

Table IV. Rotational and Hyperfine Interaction Parameters Obtained for Ar_3–H/DF by Fitting the Line Centers Listed in Tables I and II and the Hyperfine Components Given in Table III for the $K = 0$, $J = 1 \rightarrow 2$ Transitions[a]

species	B_0, MHz	D_J, kHz	D_{JK}, kHz	D_c/χ_c, kHz	θ, deg
Ar_3–HF	1188.2123 (2)	6.846 (3)	−5.753 (6)	101.6 (15)[b]	41.0 (2)
Ar_3–DF	1180.3785 (3)	6.566 (4)	−5.142 (6)	174.5 (35)[b]	35.6 (4)

[a] Numbers in parentheses are the standard deviation in the last digit(s) of the fit. [b] The value given for the HF species is D_c and that for DF is χ_c; D_c was also fitted for DF, giving a consistent but less accurate value of θ.

basically by the dipole–dipole interaction D_c, which we obtained from the hfs of the $K = 0$, $J = 1 \rightarrow 2$ transition, the assignment of which is not in doubt. In particular, if the hfs observed at 9504.359 MHz and assigned to $K = \pm 3$ were actually for $K = \pm 1$ or ± 2, it would look like the stick hfs shown for that state in Figure 1, whatever the correct D_{JK} and location of the transition. Instead, it looks like that predicted for $K = \pm 3$ and is in the position predicted on that basis, which confirms the assignment given. Moreover, there is no evidence in the observed spectrum for the $K = \pm 1$ or ± 2 states, confirming the absence of $|K| > 0$ states except those which are an integral multiple of three.

Composition and Geometry of the Clusters. Before taking up the question of interatomic distances in the clusters, it is desirable to summarize the evidence for their composition and geometry. First of all, disappearance of the transitions when either argon or H/DF is removed from the gas mixture indicates that the clusters contain both Ar and H/DF. The fact that the clusters are undoubtedly symmetric tops shows they have a threefold or higher axis of symmetry. The hyperfine structure, especially that of the $K = 0$, $J = 1 \rightarrow 2$ transitions, proves the presence of a single H/DF oriented along but making large amplitude (~40°) torsional oscillations with respect to the principal (c) axis. Hyperfine interactions from nuclei other than those within the H/DF appear to be absent.

The principal axis of the cluster is a threefold axis, interchanging three identical spin-zero nuclei. This is shown by the observation of only two nonzero K states, which are best assigned as integral multiples of three ($K = \pm 3, \pm 6$), and confirmed by the hfs of the transition assigned as $K = \pm 3$, $J = 3 \rightarrow 4$ for the HF cluster. The simplest species meeting all of these criteria is Ar_3–H/DF where the Ar_3 is an equilateral group perpendicular to the threefold axis on which the H/DF lies, as sketched in Figure 2. In principle, an Ar_4–H/DF pentamer, with the fourth Ar of the tetrahedral Ar_4 on the threefold axis, is another possibility. However, it is ruled out by the inertial analysis given in the next section which also establishes that the H/D end of H/DF is closest to the Ar_3. Furthermore, the inertial analysis gives reasonable dimensions for the proposed composition and geometry.

Inertial Analysis. Quantitative structural information for the clusters is obscured by their internal mobility as well as by the limited number of rotational constants available for a symmetric top. The cluster has nine vibrational modes. Of these, the angle-bending modes probably have the largest amplitude and the greatest effect upon B_0. The amplitude of the doubly degenerate H/DF torsion has been obtained from the hfs (Table IV). Another angular mode, also doubly degenerate, is tilt of an otherwise rigid Ar_3 group. The tilt may be described as rotation of the C_3 axis of the equilateral Ar_3 about the c axis of the complex at a fixed angle γ, as shown in Figure 2. This approximation neglects the associated motion of the H/DF just as the customary analysis of H/DF torsion neglects the Ar_3 vibration associated with it. For a symmetric top the effects of the tilt are not distinguishable from a change in the Ar–Ar distance r.

Treating the cluster as a pseudodiatomic species made up of Ar_3 and H/DF in the configuration of Figure 2, one obtains via the parallel axis theorem the following expression for its moment of inertia[15]

$$I_B = I_{bb}(Ar_3) + \tfrac{1}{2}\langle 1 + \cos^2\theta\rangle I_0(H/DF) + \mu_c R^2 \quad (6)$$

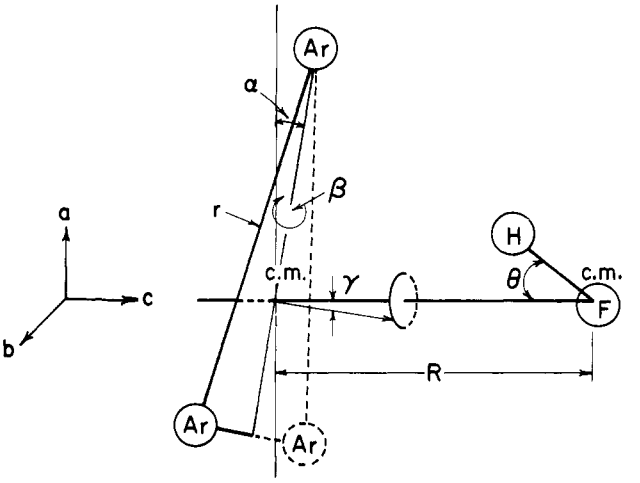

Figure 2. Geometrical structure and inertial axes of the Ar_3–HF cluster. The atomic positions in the symmetric top are drawn to scale; θ is the "average" angle between the figure (c) axis and the HF direction. The equilateral Ar_3 group is projected to indicate tilt of its plane by the angle γ from perpendicular to the c axis.

Here $I_0(H/DF)$ is the moment of inertia for free HF or DF,[9] μ_c is the pseudodiatomic reduced mass, R is the distance between the Ar_3 and H/DF centers of mass (c.m.), and $I_{bb}(Ar_3)$ is the moment of inertia for the Ar_3 about an axis parallel to the b axis of the complex and passing through the c.m. of Ar_3. In our inertial calculations, a conversion factor of 505379.0 amu Å^2 MHz was used for $I_B B_0$. $I_{bb}(Ar_3)$ may be expressed in terms of the tilt angle γ and the moments of inertia for free Ar_3 as

$$I_{bb}(Ar_3) = I_B(Ar_3)\langle 1 + \tfrac{1}{2}\sin^2\gamma\rangle = (m_{Ar}r^2/2)\langle 1 + \tfrac{1}{2}\sin^2\gamma\rangle \quad (7)$$

where

$$I_B(Ar_3) = I_A(Ar_3) = m_{Ar}r^2/2 = \tfrac{1}{2}I_C(Ar_3) \quad (8)$$

Equation 7 was obtained by calculating the effects upon $I_{gg}(Ar_3)$ (g = a, b, c) of small independent rotations α and β of the Ar_3 with respect to the a and b axis (Figure 2). The rotations are equivalent to degenerate vibrations of the form $(2d_1–d_2–d_3)$ and $(d_2–d_3)$. They increase $I_{bb}(Ar_3)$ in the cluster by displacing some of $I_A(Ar_3)$ and $I_B(Ar_3)$ with the twofold larger $I_C(Ar_3)$.

If isotopic substitution of D for H in the cluster did not affect its structure, the values of I_B observed for the two species could be used to separate their dependence upon R and r. For example, Kraitchman's isotope substitution method could be used to determine the distance of the H/D from the c.m. of the complex and thereby give R. However, this does not work because of the difference in torsional amplitudes for HF vs. DF. There is also the possibility that the Ar_3 c.m. to F distance is different for HF and DF, as in the Ar–H/DF dimer where the distance for DF is 0.010 Å shorter than that for HF. Nonetheless, eq 6 and 7 can be used to develop approximate dimensions for the cluster based upon the reasonable assumption that $I_{bb}(Ar_3)$ is affected negligibly by H/DF substitution.

In this event, by introducing the experimental values for I_B and θ (from Table IV) and for I_0[9] into eq 6 for DF and HF and subtracting, we find

$$\Delta I_B(\text{obsd, corrected for torsion}) = \mu_c'(R - \Delta R)^2 - \mu_c R^2 \quad (9)$$

where the prime indicates properties for the DF complex and $\Delta R \equiv R - R'$ is the difference in c.m. positions for the H/DF in the complexes, as projected on the c axis. If the H/DF are projected

(15) Read, W. G.; Campbell, E. J.; Henderson, G. *J. Chem. Phys.* **1983**, *78*, 3501.

(16) Colbourn, E. A.; Douglas, A. E. *J. Chem. Phys.* **1976**, *65*, 1741. See also: Godfried, H. F.; Silvera, I. F. *Phys. Rev. Lett.* **1982**, *48*, 1337.

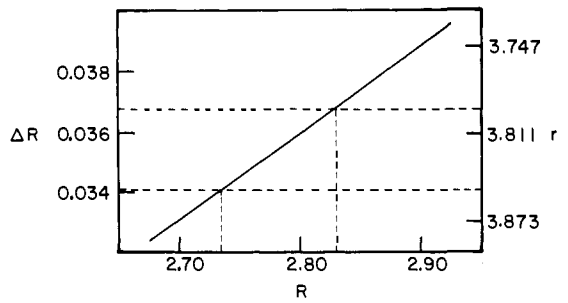

Figure 3. Plot of interatomic distances in Å consistent with the I_B's observed for Ar_3–HF and Ar_3–DF (solid line). R is the Ar_3 c.m. to HF c.m. distance, $R - \Delta R$ is the corresponding value for Ar_3–DF, and r is the Ar–Ar distance in a rigid equilateral Ar_3. The dashed lines indicate the probable range of ΔR and the associated values for R and r; the lower value of ΔR is considered more likely.

Table V. Comparison of the H/DF Torsional Amplitudes θ Observed for Ar_m–H/DF

m	Ar_m–HF, deg	Ar_m–DF, deg	θ_{HF}/θ_{DF}[a]	source
1	41.6	33.5	1.242	ref 9
2	40.7[b]	35.0[b]	1.163	ref 6
3	41.0	35.6	1.152	herein

[a] For a purely mass effect this ratio should be $(\mu_{DF}/\mu_{HF})^{1/4} = 1.175$. [b] An average of the anisotropic torsion.

at the angles θ and θ' with the fluorines at the same position along c, the magnitude of ΔR is found to be 0.0368 Å, positive if the H/D end is closest to the Ar_3 and negative if farthest from it. Given the numerical values for $\Delta I_B(cor)$, μ_c', and μ_c, eq 9 predicts the Ar_3 c.m. to HF c.m. distance R to be 2.83 Å for a positive ΔR of 0.0368 Å and 1.04 Å for a negative ΔR. A value of 2.83 Å is physically reasonable for R but 1.04 Å is not. Moreover, similar relative values of R are found for the opposite signs of ΔR over a wide range in its magnitude (0.03–0.04 Å). Therefore we conclude that the H/DF is oriented in the cluster with the H/D end closest to the Ar_3, as found in Ar–H/DF[9] and Ar_2–H/DF.[6]

The value of R found from ΔR via eq 9 is related to $I_{bb}(Ar_3)$ by eq 6 for the complex with HF. However, if the tilt of the Ar_3 is neglected, $I_{bb}(Ar_3)$ becomes simply $(m_{Ar}r^2/2)$, giving a value for the Ar–Ar distance r in the trimer. The resulting relations between ΔR, R, and r are shown graphically in Figure 3 for values of ΔR in the neighborhood of +0.0368. We consider the latter to be an upper bound to ΔR because it seems likely that the Ar_3 c.m. to F distance R_0 is somewhat *shorter* (~0.003 Å) for the HF complex than for the DF, which would reduce ΔR by the same amount. The reasons for this view follow.

The torsional amplitudes θ of the H/DF in Ar_m–H/DF are summarized in Table V for m = 1, 2, 3. As was noted above the ratio of the torsional angles $\rho \equiv \theta_{HF}/\theta_{DF}$ is 1.242 for Ar–H/DF compared with 1.175 predicted for a mass effect alone, a difference of 0.067. Moreover, R_0 for Ar–DF is 0.010 Å shorter than that for Ar–HF,[9] suggesting that the larger than predicted ρ is associated with the shorter R_0(DF). The plausibility of this is supported by the results for Ar_2–H/DF[6] in which ρ is slightly smaller than the mass effect, 1.163 vs. 1.175, and R_0(HF) is about 0.001 Å shorter than R_0(DF). The ratio of torsional angles is even smaller (1.152) for Ar_3–H/DF, differing from a pure mass effect by −0.023. Scaling the ΔR_0 in Ar–H/DF we estimate that in Ar_3–H/DF it is (−0.023/0.067)(0.010 Å)(2.75/3.50) = −0.0027, where (2.75/3.50) = $R_0(Ar_3$–HF)/R_0(Ar–HF).

With this adjustment, ΔR for Ar_3–H/DF is reduced from 0.0368 to 0.0341 Å. This corresponds, as shown graphically in Figure 3, to an Ar_3 c.m. to HF c.m. distance R of 2.735 Å and an Ar–Ar distance r of 3.850 Å, neglecting tilt. If tilt of 7.3° is included, as found for the Ar_2 torsion in Ar_2–HCl,[7] it causes a decrease via eq 7 of 0.015 Å in r, giving 3.835 Å. This is in close agreement with the 3.844 Å obtained for Ar_2–H/DF and the 3.821 Å for the free Ar_2 dimer from the B_0 of 0.05778 cm^{-1} reported for it.[6] The values of 2.735 and 3.835 Å for R and r correspond to an Ar to HF c.m. distance d of 3.519 Å, which agrees exceptionally well with the analogous distances of 3.510 Å in Ar–HF[9] and 3.519 Å in Ar_2–HF.[6]

The close similarities in interatomic distances for the Ar_m–H/DF species so far studied and in the orientation and torsional amplitudes of the H/DF in them confirm our conclusion that the species in quesion here is indeed the Ar_3–H/DF cluster as shown in figure 2. In principle the same type of symmetric top spectrum would be generated by a tetrahedral Ar_4 cluster with the H/DF on a threefold axis, the H/D end attached to either a face or apex of the tetrahedron ($ArAr_3$–H/DF or Ar_3Ar–H/DF). However, B_0 for either configuration would be much smaller than the 1185 MHz actually found. $ArAr_3$–HF would have the larger B_0, but even for it, reasonable Ar–Ar and Ar–HF c.m. distances of 3.8 and 3.5 Å lead to a predicted B_0 of ~625 MHz.

Intracluster Forces. Information about the forces within the cluster is limited to the centrifugal distortion constants D_J and D_{JK} and the torsional amplitudes of the H/DF as inferred from the hfs. D_{JK} depends on several of the force constants, so little can be inferred from it. However, as may be noted in Townes and Schawlow,[12] oblate symmetric top molecules (which are of the type XY_3) have a negative D_{JK} while molecules with a methyl group or its derivatives (which are prolate) have a positive D_{JK}. Thus, the negative values of D_{JK} we obtain for the Ar_3–H/DF clusters imply that the clusters should be oblate tops, which is indeed the case for the structures found in the inertial analysis.

If torsion of the HF is treated as a two-dimensional isotropic harmonic oscillation,[9] its amplitude θ is given by

$$\theta^2 \cong \hbar/(I_{HF}k_t)^{1/2} \tag{10}$$

where k_t is an effective force constant for the torsion. In Table V it is seen that θ is remarkably constant for the HF species, being 41.6, 40.78, and 41.0° respectively for the complexes with Ar, Ar_2, and Ar_3. This gives a range of only 9% in k_t. However, for DF there is an appreciable systematic trend, 33.5, 35.0, and 35.6°, corresponding to a decrease in k_t by 28% on going from Ar–DF to Ar_3–DF.

Stretching force constants have been obtained for many weakly bound dimers from the centrifugal distortion constant D_J, usually by a pseudodiatomic approximation[17] in which each monomer is treated as a point mass at its c.m. separated from the c.m. of the other by R. However, this approach is unsatisfactory unless the moments of inertia for both monomers are small. Several approaches[15,18] have been used to overcome this limitation. Read et al.[15] in their study of the benzene–HCl symmetric top used the expression

$$k_s = 64\pi^3(\mu_{PD}R)^2B^4/\hbar D_J \tag{11}$$

where k_s is the force constant associated with stretching R and μ_{PD} is the reduced mass of the complex viewed as a pseudodiatomic species. Their derivation treats the benzene as a rigid body, the sixfold axis of which is colinear with the HCl molecule, a rigid rod.

In our symmetric top the two "monomers" are Ar_3 and the H/DF. The Ar_3 is relatively large and massive; moreover it is held together very weakly[6,16] and must be far from rigid. The experimental values for B_0 and D_J in Table IV lead via eq 11 to a k_s of 0.332 × 10^{-5} dyn/Å for Ar_3–HF and 0.357 for Ar_3–DF. These results are much smaller than the 1.47 and 1.79 × 10^{-5} dyn/Å found for k_s in Ar–H/DF[6,9] and 1.86 and 1.97 × 10^{-5} dyn/Å in Ar_2–H/DF.[6] They serve primarily to confirm the deficiencies of the model used for the symmetric top calculation. The results for k_s, with a Lennard-Jones potential, give a well depth of only ~20 cm^{-1}, which is inconsistent with the observed signal strengths.

Discussion

The interpretation presented above of the symmetric top spectra found in the argon–H/DF system appears to be self-consistent and conclusive. Certainly the species observed have three argon

(17) Balle, T. J.; Campbell, E. J.; Keenan, M. R.; Flygare, W. H. *J. Chem. Phys.* **1979**, *71*, 2723; **1980**, *72*, 922.
(18) Millen, D. J. *Can. J. Chem.* **1985**, *63*, 1477.

Table VI. Comparison of Structural Parameters Found for Ar_m–HF (m = 1, 2, 3) Averaged over the HF Torsion[a]

species	R, Å	d_0, Å	r, Å	source
Ar–HF	3.510	3.557	–	ref 8 and 9
Ar_2–HF	2.986	3.584	3.823	ref 6
Ar_3–HF	2.735	3.566	3.835	herein

[a] The distances are the following: R, Ar_m c.m. to HF c.m.; d_0, Ar–F; r, Ar–Ar.

atoms and a single H/DF molecule in a vibrationally averaged toadstool structure with the H/DF along a threefold axis of symmetry, the H/D end closest to the Ar_3. This is supported not only by the hfs and centrifugal splitting of the $\Delta J = 1$ transitions but also by the interatomic distances in the clusters, which are very similar to those found for Ar–H/DF and Ar_2–H/DF.

The sequence of geometrical structures for the complexes of H/DF with Ar, Ar_2, and Ar_3 is noteworthy. The interaction of Ar with H/DF does not appear to be highly localized. If it were, one might find, for example, complexes with Ar_2 in which the H/DF is attached preferentially to a single Ar giving a linear or bent Ar–Ar–H/DF. Also, by analogy with the T-shaped Ar_2–HF, the Ar_3–HF might be planar with the H/DF attached to an edge of the Ar_3 triangle. Instead, the actual structures of the clusters are determined primarily by the structure of the Ar_m portion, with the H/DF located so that it interacts symmetrically with the argon atoms available. Ar_2–H/DF is planar and T-shaped, with C_{2v} symmetry.[6] Its asymmetric top spectrum enabled us to measure for it the modest anisotropy in the torsional motions of the H/DF, which are ~3° larger in-plane than out-of-plane (32.8° vs. 29.7° for HF). Its smallness suggests that the potential function for the H/DF has a single minimum located on the c axis. Moreover, no other effects of the anisotropy in the potential function were noted.

The symmetric top structure observed for Ar_3–H/DF is an average over the torsional motions of the H/DF. However, as in the similar case of the benzene–HCl complex,[15] there are two types of potential functions that can average to a symmetric top. The equilibrium structure could have a single axially symmetric minimum with the H/DF pointed directly at the Ar_3 c.m. (θ_e = 0°) or it could have three equivalent minima with the H/DF pointed at or near one of the argons ($\theta_e \sim 39°$ for Ar_3–HF). In the latter event, depending upon the barriers between the three minima and their shape, the hydrogen atom of the H/DF would undergo hindered internal rotation or tunneling with respect to the argon triad. Such motions perturb the rotational energy levels and often cause readily detectable splittings in rotational spectra.[19]

No evidence of these effects was found in the present case. Small splittings of ≤10 MHz would have been found without difficulty; their absence in the $J = 3 \rightarrow 4$ transitions in Figure 1 places an upper limit of ~5 kHz on them. Larger splittings or displacements seem unlikely because of the excellent fits to a simple, symmetric top model for both the HF and DF clusters with only the expected small differences in rotational constants (Table IV). However, the effective moment of inertia for internal rotation of the H/DF is small, so any excited hindered rotor states could lie too high to be populated enough for detection in the nozzle expansion (~5 K).

The best evidence for an equlibrium structure with a single potential minimum on the threefold axis is a comparison of the torsional amplitudes found for HF and DF in the two clusters. If there were three potential minima, the torsional amplitudes of HF and DF should be very similar because both would be determined mainly by the location and shape of the minima. Instead the ratio θ_{HF}/θ_{DF} in Table V is close to that predicted as a mass effect for a simple harmonic vibration. However, the trend in the ratio, decreasing as the number of argons in the complex increases, shows that the shape of the potential minimum also changes.

Table VI summarizes the internuclear distances R, d_0, and r found for Ar_m–HF (m = 1, 2, 3). The values are corrected for the HF torsion but not for Ar_2 torsion or Ar_3 tilt (for which the data are insufficient). The large range, 3.510–2.735 Å, in the Ar_m c.m. to HF c.m. distance R is a result of the different geometries of the m = 1, 2, 3 clusters. However, the Ar to F and Ar–Ar distances, d_0 and r, are remarkably constant for the three clusters; d_0 ranges between 3.557 and 3.584 Å while r is 3.823 and 3.835 Å for the Ar_2 and Ar_3 species, respectively. The latter is slightly larger than the 3.821 Å found for the free Ar_2 dimer.[6] The results for Ar_m–HCl are very similar.[7] The main difference is that the Ar–Ar distances are about 0.02 Å larger in the Ar_2– and Ar_3–HX clusters, indicating that cluster formation lengthens r from its value in free Ar_2.

The rotational spectrum of the cluster partially substituted with ^{36}Ar would provide more detailed information about its structure, particularly on the Ar–Ar distance, the tilt of the Ar_3, and the force field. At natural isotopic abundance, about 1% of the clusters would be $^{36}Ar^{40}Ar_2$–HF. However, the intensity is spread over three to four times as many transitions as for the symmetric top. Our efforts to detect it have been unsuccessful so far, but with recent and scheduled further improvements in sensitivity, we may find it. The same can be said about the next larger cluster, Ar_4–HF, for which the most likely Ar_4 configuration is a tetrahedron, though it might be a diamond. Further search for the pentamer is also planned.

Acknowledgment. We thank Cliff Dykstra for several stimulating and helpful discussions. This work was supported by a Charles W. Walton Research Grant, by the University of Illinois Campus Research Board, by the School of Chemical Sciences, and by the National Science Foundation. Acknowledgement is made to the donors of the Petroleum Research Fund, administered by the American Chemical Society, for partial support of this research.

(19) Gordy, W.; Cook, R. L. *Microwave Molecular Spectra*; Interscience: New York, 1970; Chapter 12.